



# Mechanical behavior of Al–Zn–Mg–Cu alloy under tension in semi-solid state

Gang CHEN<sup>1</sup>, Yu-min ZHANG<sup>2</sup>, Zhi-ming DU<sup>1</sup>

1. School of Materials Science and Engineering, Harbin Institute of Technology at Weihai, Weihai 264209, China;

2. School of Astronautics, Harbin Institute of Technology, Harbin 150001, China

Received 9 April 2015; accepted 12 October 2015

**Abstract:** In order to study the hot fractures in relation to the semi-solid processing, the tensile tests of an extruded 7075 aluminum alloy which is based on Al–Zn–Mg–Cu system were carried out in the high temperature solid and semi-solid states at different strain rates. The results show that the tensile behavior can be divided into three regimes with increasing the liquid fraction. The alloy first behaves in a ductile character, and as the temperature increases, the fracture mechanism changes from ductile to brittle which is determined by both of liquid and solid, and lastly the fracture mechanism is brittle which is totally dominated by liquid. At strain rates of  $1 \times 10^{-4}$ ,  $1 \times 10^{-3}$  and  $1 \times 10^{-2} \text{ s}^{-1}$ , the brittle temperature ranges are 515–526, 519–550 and 540–580 °C, respectively. Two equations which are critical for tensile behavior are proposed.

**Key words:** Al–Zn–Mg–Cu alloy; mechanical behavior; semi-solid processing; fracture

## 1 Introduction

The Al–Zn–Mg–Cu alloys have great age hardening response, and are the strongest wrought aluminum alloys. The fine strengthening precipitates ( $\text{MgZn}_2$  and  $\text{Al}_2\text{Mg}_3\text{Zn}_3$ ), which form in the decomposition of a super-saturated solid solution during aging treatment, are responsible for the high performance of Al–Zn–Mg–Cu alloys [1]. These alloys such as 7075 aluminum alloys are widely used for aerospace applications, and usually shaped by extensive machining from the wrought state with much wastage. Therefore, it has great practical significance to process Al–Zn–Mg–Cu alloys in near net shape.

Semi-solid metal processing (SSP) is a promising and powerful near net shaping route for forming alloys or metal matrix composites in the semi-solid state [2]. The materials must have an appreciable melting range and the microstructures must consist of non-dendritic solid metal spheroids in a liquid matrix before SSP [3–5]. The technology could process components with complex shape and high mechanical properties which are nearly as good as those in wrought parts [6–9]. Recently, increasing attention has been given to semi-solid

processing of Al–Zn–Mg–Cu alloys and other wrought aluminum alloys, and some 7xxx series aluminum alloys (based on the Al–Zn–Mg–Cu system) have been shown to be potential for semi-solid processing [10,11]. However, the Al–Zn–Mg–Cu alloys generally have wide freezing ranges, thus tending to be hot tearing [12]. Tensile stress or strain is the essential responsible for the hot fracture behavior. Therefore, studying the tensile mechanical behavior of semi-solid Al–Zn–Mg–Cu alloys is the most direct and effective route to understand the hot tearing during semi-solid processing.

The measured stresses and strains are small in the semi-solid state, so tensile tests are usually difficult to be carried out. Nevertheless, there are still some studies which focus on the tensile behavior of as-cast aluminum alloys related to direct chill casting [13–20].

FABRÈGUE et al [15] studied the mechanical properties of Al–Mg–Si–Cu alloys in the mushy state. Unlike other work which was conducted by reheating solid alloys into the semi-solid state, they studied the tensile behavior during solidification which was in relation to the phenomenon of hot tearing. PHILLION et al [16–20] studied the semi-solid constitutive behavior and hot tearing of a series of aluminum and magnesium alloys, and have made great achievement in these fields.

**Foundation item:** Project (51405100) supported by the National Natural Science Foundation of China; Project (2014M551233) supported by the Postdoctoral Science Foundation of China; Project (2014-HT-HGD12) supported by the Astronautical Supporting Technology Foundation of China; Project (2015GGX102023) supported by the Plan of Science and Technology Development in Shandong Province, China

**Corresponding author:** Gang CHEN; Tel: +86-631-5687324; E-mail: [gangchen@hit.edu.cn](mailto:gangchen@hit.edu.cn)

DOI: 10.1016/S1003-6326(16)64153-5

They proposed a novel semi-solid tensile deformation methodology combined with X-ray micro-tomography, in order to investigate the porosities and hot tearing [16,17]. They found that the as-cast porosity is intimately linked to the hot tearing susceptibility of aluminum alloys. Besides, PHILLION et al [18] measured the tensile mechanical response of three semi-solid as-cast aluminum alloys (AA3104, AA6111 and CA31218), so as to establish the mushy zone constitutive behavior and propose a brittle temperature range for each of the three alloys. A direct finite-element microstructure model was proposed to predict the deformation behavior of semi-solid metallic alloys [19]. HU et al [20] studied the constitutive behavior of as-cast magnesium alloy Mg–3Al–1Zn in the semi-solid state, and obtained an equation relating the maximum tensile stress with temperature.

However, little work has been done to study the tensile behavior in relation to the semi-solid processing. In the previous work, a preliminary study about the tensile behavior of Al–Zn–Mg–Cu alloy was carried out [21]. The tensile tests were performed at different temperatures and strain rate of  $1 \times 10^{-3} \text{ s}^{-1}$ , but the comprehensive effects of temperature (liquid fraction) and strain rate on the tensile behavior have not been analyzed thoroughly.

In this research, hot tensile tests were carried out on an extruded 7075 aluminum alloy (based on the Al–Zn–Mg–Cu system) in the high temperature solid and semi-solid states, in order to determine the tensile stresses and strains that can be sustained by semi-solid 7075 aluminum alloy at different liquid fractions and strain rates. Studying the tensile behavior of 7075 aluminum alloy in the semi-solid state will improve the understanding of hot fractures related to semi-solid processing, and enable the optimization for practical application.

## 2 Experimental

The commercially wrought 7075 aluminum alloy used was supplied in the form of extruded rods with 55 mm in diameter and composition of Al–5.84Zn–2.17Mg–1.41Cu–0.20Cr–0.22Mn (mass fraction, %). These rods were then extruded to 13 mm in diameter at 400 °C with an extrusion ratio of 17:1. Cylindrical tensile specimens with a gauge length of 120 mm and a diameter of 10 mm were machined from the extruded rods with their long axis paralleling to the extrusion direction. Each specimen contained a central reduced region ( $l=20 \text{ mm}$ ,  $d=5 \text{ mm}$ ), as shown in Fig. 1.

Differential scanning calorimetry (DSC) was used to determine the solidification interval and the liquid fraction–temperature relationship. The samples with

3 mm in diameter and mass of about 30 mg were heated to 700 °C at 10 °C/min and cooled to room temperature at the same rate. Figure 2 shows the change in liquid fraction with temperature obtained from the heat flow versus temperature curve. During reheating, there are some reactions would form liquid in sequence [1]. The first precipitates to form liquid are the submicron sized  $\text{MgZn}_2$  and  $\text{Al}_2\text{Cu}$  at the solidus temperature (around 470 °C).

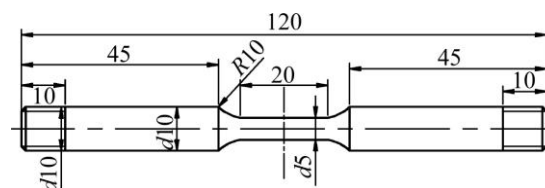


Fig. 1 Schematic diagram of tension specimens (unit: mm)

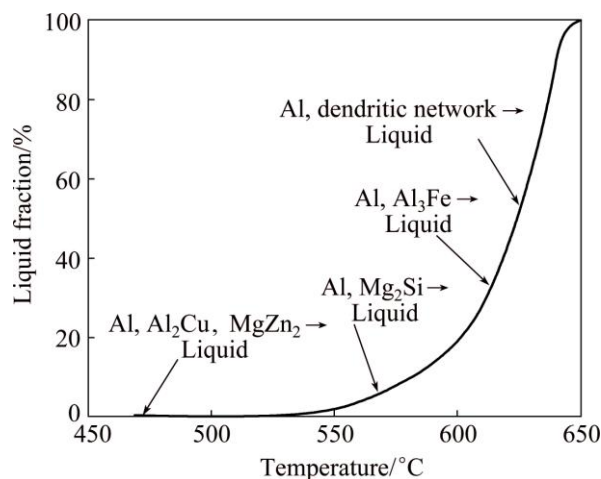


Fig. 2 Liquid fraction vs temperature curve of 7075 aluminum alloy

The semi-solid tensile tests were performed using a Gleeble 1500 thermomechanical simulator. The tensile specimens were reheated at 100 °C/min via Joule heating, and isothermally held for 1 min on reaching the target temperature. According to the recrystallisation and partial melting (RAP) route [22], recrystallisation occurs in the extruded materials during the reheating, and as liquid forms, the liquid penetrates the recrystallized boundaries to form the spheroids suitable for semi-solid processing. The temperature was controlled by two thermocouples which were first welded on the specimens and then fixed using high-temperature adhesive which consists of two components based on ceramic material. Tensile tests were conducted from 400 to 580 °C at strain rates of  $1 \times 10^{-4}$ ,  $1 \times 10^{-3}$  and  $1 \times 10^{-2} \text{ s}^{-1}$ , respectively. For the tensile sample, the diameters of clamping region and gauge region are  $d10 \text{ mm}$  and  $d5 \text{ mm}$ , respectively. Therefore, the heat generated by Joule heating in the gauge region is higher than that in the clamping region.

During tension testing, when the gauge region is in the semi-solid state, the temperature of clamping region is much lower with higher strength. Therefore, the tensile sample will not rupture at the clamping position. During testing, the temperature is relatively uniform for the length of 15 mm in the gauge region, so the initial gauge length is set to be 15 mm. The force  $f$  and current length  $L$  of the gauge region were recorded. The true strain was derived based on standard equation  $\varepsilon = \ln(L/L_0)$ , where  $L_0$  is the initial length. The true stress  $\sigma$  was derived based on equation  $\sigma = 4f/(\pi D^2)$ , where  $D$  is the current diameter obtained from volume constancy. After tensile testing, the specimens were sectioned for electron fractography.

### 3 Results and discussion

Figure 3 shows the variation of ultimate tensile stress (UTS) and failure strain as a function of temperature at different strain rates. The UTS and ductility all decrease with increasing the temperature, but the decreasing rates are not synchronous. As shown in Fig. 3(a), when the temperature increases from the high temperature solid state into the semi-solid state with a small amount of liquid present (below 500 °C), both the UTS and failure strain decline slowly at a strain rate of  $1 \times 10^{-4} \text{ s}^{-1}$ , and then decrease sharply as the temperature increases. At 526 °C onwards, the UTS almost keeps stable. Nevertheless, the failure strain decreases to a relative stable value at 515 °C, and actually the material almost loses all ductility. As shown in Fig. 3(b), the tensile behavior of 7075 aluminum alloy at a strain rate of  $1 \times 10^{-3} \text{ s}^{-1}$  is similar to that at  $1 \times 10^{-4} \text{ s}^{-1}$ . The temperatures at which the UTS and failure strain decrease to relatively stable values are 550 and 519 °C, respectively. When the strain rate increases to  $1 \times 10^{-2} \text{ s}^{-1}$ , the tensile behavior shows a little difference, as shown in Fig. 3(c). The UTS almost decreases linearly as the temperature increases, and the failure strain firstly declines linearly until 540 °C, and then nearly keeps stable.

At high temperatures, when the failure strain is almost stable at a minimal value of  $\sim 0.01$ , the UTS of this alloy is still 20–25 MPa. Actually, the UTS is influenced by the adhesive, which was used to fix the thermocouples on the tensile specimens. Therefore, the true UTS is a little lower than the experimental value [20]. The alloy can be thought to have nearly lost the tensile strength yet.

In the semi-solid state with small liquid fraction, the liquid exists as isolated pocket and has almost no effect on the constitutive behavior. Therefore, the variation of UTS and failure strain with increasing the temperature is similar to that in the high temperature solid state. As the temperature increases, the liquid pockets begin to

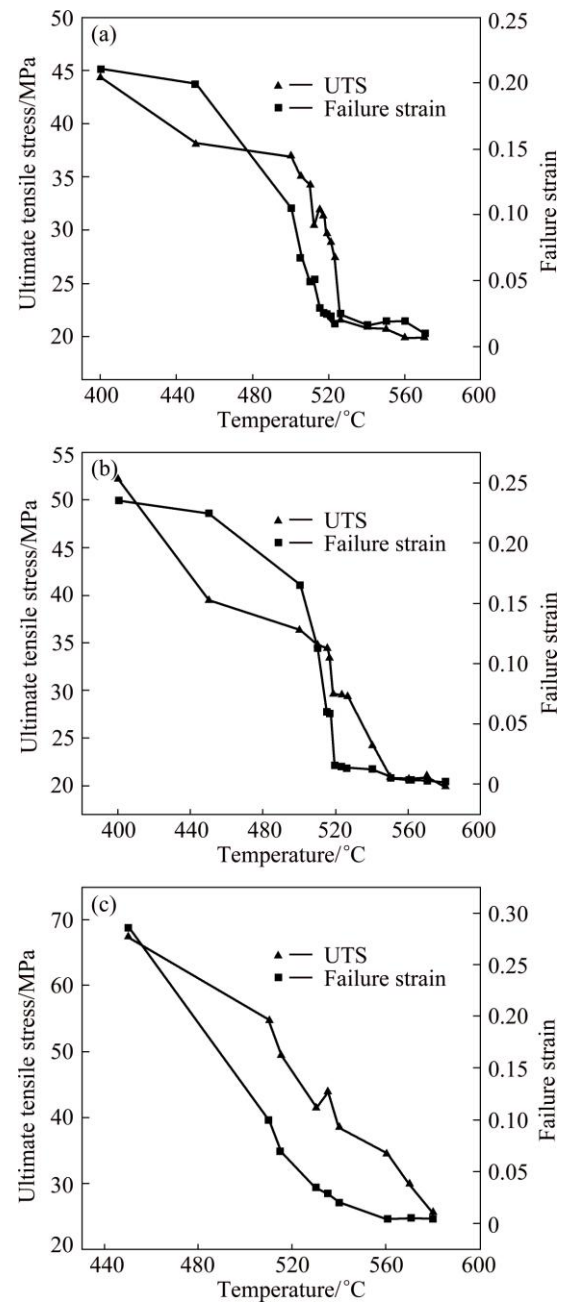


**Fig. 3** Variation of UTS and failure strain as function of temperature at strain rates of  $1 \times 10^{-4} \text{ s}^{-1}$  (a),  $1 \times 10^{-3} \text{ s}^{-1}$  (b) and  $1 \times 10^{-2} \text{ s}^{-1}$  (c)

combine together to form a continuous film around the grains, leading to a rapid decline in the mechanical properties. When the liquid films are large enough to isolate the solid particles from each other, the alloy would hardly sustain any tensile strain.

The two temperatures when the alloy almost loses all ductility and cannot sustain any tensile stress are termed as the critical ductility temperature and the critical stress temperature, respectively. The region between these two critical temperatures is termed as the brittle temperature range, in which the material can still

sustain some stress but with little ductility. Therefore, the alloy exhibits large hot tearing probability in the brittle range. As shown in Fig. 3, the brittle temperature ranges are 515–526, 519–550 and 540–580 °C when the strain rates are  $1 \times 10^{-4}$ ,  $1 \times 10^{-3}$  and  $1 \times 10^{-2} \text{ s}^{-1}$ , respectively. Considering the influence of adhesive, the accurate upper limit of the brittle range may be a little lower. When the strain rate increases from  $1 \times 10^{-4}$  to  $1 \times 10^{-2} \text{ s}^{-1}$ , the critical temperatures increase evidently, and the brittle ranges also become wider. As the strain rate increases, there is not enough time for the liquid phase to spread along the micro-cracks, so the strength of alloy increases with increasing the strain rate. The influence of strain rate on the strength is stronger than that of ductility resulting in wider brittle ranges as the strain rate increases.

Figure 4 shows the fracture surface morphologies of tensile specimens tested at different temperatures and a strain rate of  $1 \times 10^{-3} \text{ s}^{-1}$ . The macroscopic observation with a low magnification is presented in lower left corner of each figure, and the microscopic view is corresponding to the square region. As shown in Fig. 4(a) (at 510 °C), most of the fracture surfaces are dominated by complex topography showing typical ductile fracture features, and a small smooth region appears at the bottom, indicating partial melting of surface. Some cleavage platforms, tearing ridges and a few dimples exist in the square region, showing that the fracture is a

mixture of cleavage and tearing, which is between brittle and ductile.

When the test temperatures are higher (at 523 and 550 °C), the fracture surfaces all consist of two different morphologies, as shown in Figs. 4(b) and (c). One part shows typical intergranular fracture features which turn from ductile to brittle. Another part is totally covered by a smooth plate showing that the liquid dominates the fracture behavior, and the liquid area increases as the temperature increases.

As shown in Fig. 4(d), the fracture surface entirely consists of fine equiaxed grains at 580 °C, which indicates that the whole fracture surface is covered by a liquid film. The liquid phase dominates the fracture behavior at this temperature, which is consistent with the loss of capacity to withstand tensile stress.

Based on the tensile results and electron fractographies, the tensile mechanical and fracture behaviors of as-deformed Al–Zn–Mg–Cu alloy can be divided into three regimes from the high temperature solid state to the semi-solid state. The alloy firstly behaves in a predominantly ductile character which is similar to that of fully solid material, and the liquid has little effect on the tensile behavior. As the temperature and the liquid fraction increase, the liquid phase plays a more important role in the tensile behavior, and the fracture mechanism turns from ductile to brittle. At a higher temperature with more liquid present, the tensile

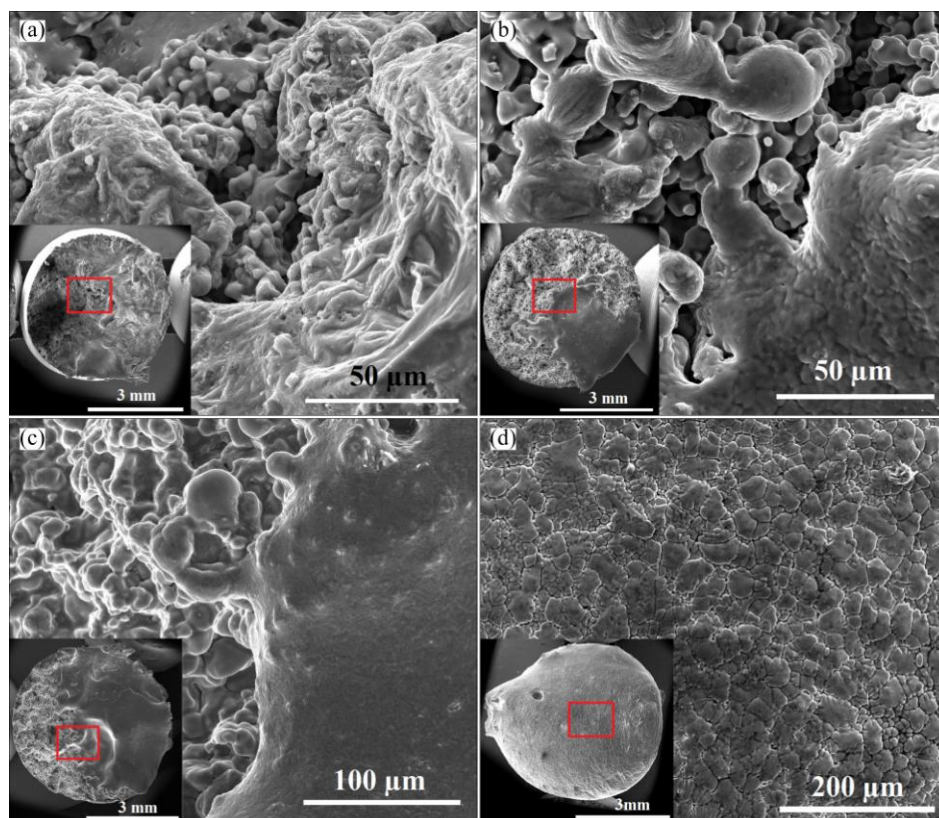


**Fig. 4** Fracture surface morphologies of semi-solid tension specimens tested at 510 °C (a), 523 °C (b), 550 °C (c) and 580 °C (d) under strain rate of  $1 \times 10^{-3} \text{ s}^{-1}$



behavior is totally dominated by liquid, and the whole fracture surface is covered by liquid phase, showing that the alloy completely loses the capacity to withstand tensile stress.

LAHAIE and BOUCHARD [23] proposed a numerical constitutive model for semi-solid Al alloys when it is in the liquid film stage, and they assumed that the two-dimensional cut of solid grains is in the form of regular hexagons. The mechanical response predicted by the model agrees well with some experimental data, which can be expressed as

$$\sigma = \frac{\mu \dot{\varepsilon}}{9} \left( \frac{\varphi_s^m}{1 - \varphi_s^m} \right)^3 \left\{ \left[ 1 - 1/2 \left( \frac{\varphi_s^m}{1 - \varphi_s^m} \right) \varepsilon \right]^{-3} + 2 \left[ 1 + \left( \frac{\varphi_s^m}{1 - \varphi_s^m} \right) \varepsilon \right]^{-3} \right\} \quad (1)$$

where  $\mu$  is the viscosity of intergranular liquid,  $\dot{\varepsilon}$  is the applied strain rate,  $\varepsilon$  is the accumulated strain,  $\varphi_s$  is the solid fraction, and  $m$  is a microstructural parameter (1/2 for columnar microstructure and 1/3 for equiaxed microstructure). In this work, the fracture surface of tensile specimen is covered by a liquid film at 580 °C, indicating that the semi-solid body is in the liquid film stage. Therefore, according to the numerical constitutive model proposed by LAHAIE and BOUCHARD [23], the calculated tensile strength is about 6.7 MPa at 580 °C with a strain rate of  $1 \times 10^{-3} \text{ s}^{-1}$ . Compared with the experimental data (20 MPa), the difference is caused by two reasons: the first is the influence of high-temperature adhesive, and the second is that the strain and strain rate in Eq. (1) are local ones while global strain and strain rate are used in the experiments of this work.

The tensile behaviors of semi-solid Al–Zn–Mg–Cu alloy are closely dependent on the temperature and strain rate. The variation of ultimate tensile stress with increasing the temperature and strain rate is plotted in Fig. 5. As shown in Fig. 5(a), the UTS decreases with increasing the temperature. At strain rates of  $1 \times 10^{-4}$  and  $1 \times 10^{-3} \text{ s}^{-1}$ , the variation processes can be divided into three stages according to different decreasing rates, which are consistent with the tensile behavior regimes as discussed previously. The difference between the three stages is smaller at  $1 \times 10^{-3} \text{ s}^{-1}$  compared with that at  $1 \times 10^{-4} \text{ s}^{-1}$ . At a strain rate of  $1 \times 10^{-2} \text{ s}^{-1}$ , the UTS almost decreases linearly with increasing the temperature, and the relationship can be expressed by a simple linear equation:

$$\sigma_s = -0.3125t + 208 \quad (2)$$

where  $\sigma_s$  is the UTS (MPa) and  $t$  is the temperature (°C). This equation is only valid from 400 to 580 °C. At higher strain rates, the relationship between UTS and temperature should also be linear but with different ratios.

As shown in Fig. 5(b), the UTS increases with increasing the strain rate, and the relationship between UTS and  $\lg \dot{\varepsilon}$  becomes linear gradually as the temperature increases. At 570 °C, the relationship could be expressed by a linear equation:

$$\sigma_s = 4.9 \lg \dot{\varepsilon} + 39.6 \quad (3)$$

Based on the variation trend, it is assumed that this equation may be valid from 560 °C to a slightly higher temperature. These results can be included in the simulations of semi-solid processing of Al–Zn–Mg–Cu alloys in order to predict hot fractures using stress-based criteria since the tensile behavior in the semi-solid range has been obtained [24].

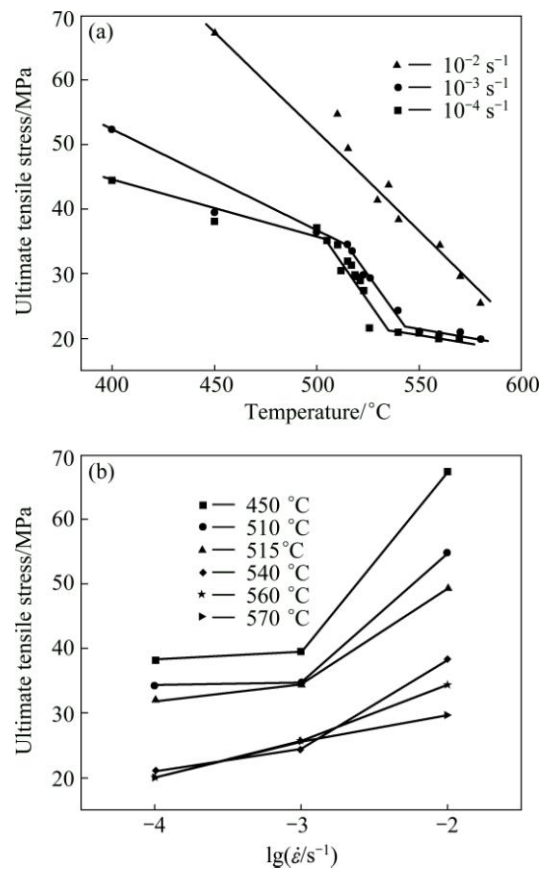


**Fig. 5** Variation of ultimate tensile stress at different temperatures (a) and strain rates (b)

## 4 Conclusions

1) The tensile behavior can be divided into three regimes based on the tensile results and electron fractographies. The alloy firstly behaves in a predominantly ductile character. As the temperature increases, the liquid phase plays a more important role in the tensile behavior, and the fracture mechanism changes from ductile to brittle. Lastly at a higher temperature, the tensile behavior is totally dominated by liquid and the alloy completely loses the capacity to withstand tensile

stress.

2) At strain rates of  $1 \times 10^{-4}$ ,  $1 \times 10^{-3}$  and  $1 \times 10^{-2} \text{ s}^{-1}$ , the brittle temperature ranges are 515–526, 519–550 and 540–580 °C, respectively.

3) Two equations which are critical for tensile behaviors are proposed. One is based on UTS and temperature, the other is based on UTS and strain rate.

## References

- [1] ATKINSON H V, BURKE K, VANEETVELD G. Recrystallisation in the semi-solid state in 7075 aluminium alloy [J]. *Materials Science and Engineering A*, 2008, 490(1): 266–276.
- [2] ATKINSON H V. Modelling the semisolid processing of metallic alloys [J]. *Progress of Materials Science*, 2005, 50(3): 341–412.
- [3] WU S S, XIE L Z, ZHAO J W, NAKAE H. Formation of non-dendritic microstructure of semi-solid aluminium alloy under vibration [J]. *Scripta Materialia*, 2008, 58(7): 556–559.
- [4] CHEN Qiang, YUAN Bao-guo, ZHAO Gao-zhan, SHU Da-yu, HU Chuan-kai, ZHAO Zu-de, ZHAO Zhi-xiang. Microstructural evolution during reheating and tensile mechanical properties of thixoforged AZ91D-RE magnesium alloy prepared by squeeze casting–solid extrusion [J]. *Materials Science and Engineering A*, 2012, 537: 25–38.
- [5] ZHAO Zu-de, CHEN Qiang, HUANG Shu-hai, CHAO Hong-ying. Microstructural evolution and tensile mechanical properties of thixoforged ZK60-Y magnesium alloys produced by two different routes [J]. *Materials and Design*, 2010, 31(4): 1906–1916.
- [6] CHEN Qiang, LUO Shou-jing, ZHAO Zu-de. Microstructural evolution of previously deformed AZ91D magnesium alloy during partial remelting [J]. *Journal of Alloys and Compounds*, 2009, 477(1): 726–731.
- [7] KIM W Y, KANG C G, KIM B M. The effect of the solid fraction on rheological behavior of wrought aluminium alloys in incremental compression experiments with a closed die [J]. *Materials Science and Engineering A*, 2007, 447(1): 1–10.
- [8] CHEN Qiang, YUAN Bao-guo, LIN Jun, XIA Xiang-sheng, ZHAO Zu-de, SHU Da-yu. Comparisons of microstructure, thixoformability and mechanical properties of high performance wrought magnesium alloys reheated from the as-cast and extruded states [J]. *Journal of Alloys and Compounds*, 2014, 584: 63–75.
- [9] CHEN Qiang, ZHAO Zu-de, ZHAO Zhi-xiang, HU Chuan-kai, SHU Da-yu. Microstructure development and thixoextrusion of magnesium alloy prepared by repetitive upsetting–extrusion [J]. *Journal of Alloys and Compounds*, 2011, 509(26): 7303–7315.
- [10] CHAYONG S, ATKINSON H V, KAPRANOS P. Thixoforming 7075 aluminium alloys [J]. *Materials Science and Engineering A*, 2005, 390(1): 3–12.
- [11] CHAYONG S, ATKINSON H V, KAPRANOS P. Multistep induction heating regimes for thixoforming 7075 aluminum alloy [J]. *Materials Science and Technology*, 2004, 20(4): 490–496.
- [12] CAMACHO A M, ATKINSON H V, KAPRANOS P, ARGENT B B. Thermodynamic predictions of wrought alloy compositions amenable to semi-solid processing [J]. *Acta Materialia*, 2003, 51(8): 2319–2330.
- [13] van HAAFTEN W M, KOOL W H, KATGERMAN L. Tensile behaviour of semi-solid industrial aluminium alloys AA3104 and AA5182 [J]. *Materials Science and Engineering A*, 2002, 336(1): 1–6.
- [14] COLLEY L J, WELLS M A, MAIJER D M. Tensile properties of as-cast aluminium alloy AA5182 close to the solidus temperature [J]. *Materials Science and Engineering A*, 2004, 386(1): 140–148.
- [15] FABRÈGUE D, DESCHAMPS A, SUERY M, DREZET J M. Non-isothermal tensile tests during solidification of Al–Mg–Si–Cu alloys: Mechanical properties in relation to the phenomenon of hot tearing [J]. *Acta Materialia*, 2006, 54(19): 5209–5220.
- [16] PHILLION A B, COCKCROFT S L, LEE P D. X-ray micro-tomographic observations of hot tear damage in an Al–Mg commercial alloy [J]. *Scripta Materialia*, 2006, 55(5): 489–492.
- [17] PHILLION A B, COCKCROFT S L, LEE P D. A new methodology for measurement of semi-solid constitutive behavior and its application to examination of as-cast porosity and hot tearing in aluminium alloys [J]. *Materials Science and Engineering A*, 2008, 491(1): 237–247.
- [18] PHILLION A B, THOMPSON S, COCKCROFT S L, WELLS M A. Tensile properties of as-cast aluminium alloys AA3104, AA6111 and CA31218 at above solidus temperatures [J]. *Materials Science and Engineering A*, 2008, 497(1): 388–394.
- [19] PHILLION A B, COCKCROFT S L, LEE P D. A three-phase simulation of the effect of microstructural features on semi-solid tensile deformation [J]. *Acta Materialia*, 2008, 56(16): 4328–4338.
- [20] HU K, PHILLION A B, MAIJER D M, COCKCROFT S L. Constitutive behavior of as-cast magnesium alloy Mg–Al<sub>3</sub>–Zn<sub>1</sub> in the semi-solid state [J]. *Scripta Materialia*, 2009, 60(6): 427–430.
- [21] CHEN G, JIANG J F, DU Z M, HAN F, ATKINSON H V. Hot tensile behavior of an extruded Al–Zn–Mg–Cu alloy in the solid and in the semi-solid state [J]. *Materials and Design*, 2014, 54: 1–5.
- [22] KIRKWOOD D H, SELLARS C M, ELIAS BOYED L G. Thixotropic materials: European Patent, 0305375 B1 [P]. 1992.
- [23] LAHAIE D J, BOUCHARD M. Physical modeling of the deformation mechanisms of semisolid bodies and a mechanical criterion for hot tearing [J]. *Metallurgical and Materials Transactions B*, 2001, 32(4): 697–705.
- [24] ESKIN D G, SUYITNO, KATGERMAN L. Mechanical properties in the semi-solid state and hot tearing of aluminium alloys [J]. *Progress of Materials Science*, 2004, 49(5): 629–711.

# 半固态 Al–Zn–Mg–Cu 合金的拉伸力学行为

陈 刚<sup>1</sup>, 张宇民<sup>2</sup>, 杜之明<sup>1</sup>

1. 哈尔滨工业大学(威海) 材料科学与工程学院, 威海 264209; 2. 哈尔滨工业大学 航天学院, 哈尔滨 150001

**摘 要:** 为了研究半固态成形过程中的热裂现象, 在高温固态和半固态及不同应变速率对 Al–Zn–Mg–Cu 系挤压态 7075 铝合金进行拉伸试验。结果表明: 随着液相率的升高, 7075 铝合金在拉伸过程中表现为 3 种变形机制。首先, 合金表现为典型的塑性变形特征; 随着温度升高, 合金的变形行为由固相和液相共同决定, 变形特点由塑性向脆性转变; 液相率更高时, 合金的变形行为完全由液相决定, 并表现为明显的脆性变形特点。在应变速率分别为  $1 \times 10^{-4}$ 、 $1 \times 10^{-3}$  和  $1 \times 10^{-2} \text{ s}^{-1}$  时, 合金的脆性温度区间分别为 515–526、519–550 和 540–580 °C。此外, 建立了关于拉伸行为的两个关键方程。

**关键词:** Al–Zn–Mg–Cu 合金; 力学行为; 半固态成形; 断裂

(Edited by Mu-lan QIN)